

# Effect of doping with chromium on the physicochemical properties of iron-molybdenum oxide systems

M. DEL ARCO, C. MARTIN, V. RIVES\*

*Departamento de Química Inorgánica, Universidad de Salamanca, Facultad de Farmacia, Avda. del Campo Charro, s/n, 37007-Salamanca, Spain*

A. M. ESTEVEZ, M. C. MARQUEZ, A. F. TENA

*Departamento de Ingeniería Química y Textil, Universidad de Salamanca, Facultad de Ciencias Químicas, Plaza de los Caídos, 1-5, 37008-Salamanca, Spain*

Iron-molybdenum oxide systems have been prepared by coprecipitation from aqueous solutions. Two sets of samples have been prepared, undoped and doped with chromium, and the results have been compared with those corresponding to a commercial catalyst now under use. The catalysts have been characterized by chemical analysis, X-ray diffraction, visible-ultraviolet (diffuse reflectance), nitrogen adsorption at 77 K for surface area and porosity and scanning electron microscopy. It has been concluded that the composition of the final solid strongly depends on the composition of the starting solutions, but that the presence of chromium does not severely affect the Mo-Fe ratio; on the contrary, the presence of chromium in the catalysts leads to an outstanding development of surface area.

## 1. Introduction

Molybdate compounds are currently being studied because of their catalytic activity for selective oxidation reactions [1, 2]. Although pure molybdates are sometimes investigated, most of the catalysts used are mixtures of molybdates and molybdena, i.e., the molybdate itself with an "excess" of MoO<sub>3</sub> [2]. There is a huge number of papers in the literature concerning the preparation, characterization, acidic properties, etc. of these systems, as well as on the role played by different crystal faces of the catalyst on the catalytic activity, and on their activity and selectivity in propene, C<sub>4</sub> hydrocarbons, methanol, etc. oxidation processes [3, 4].

Mixed oxides of iron and molybdenum are used in industry for oxidation of methanol to formaldehyde as these catalysts are very resistant to poisoning and are highly selective in the mentioned reaction [5-8]. The use of this type of catalyst was first reported by Adkins and Peterson in the early thirties [9], although only from the fifties have they partly displaced the use of silver-based catalysts for formaldehyde production on an industrial scale. Although other catalysts, such as molybdenum bismuth oxides [10], molybdenum and antimony oxides [11], unloaded molybdena [12] or supported on silica [13, 14] or even zeolites [15], have been reported to be effective in this reaction, it seems that from the commercial point of view the so-called "FeMo" catalysts are still far ahead.

As mentioned above, better results are generally obtained when the amount of molybdenum in the catalyst exceeds that corresponding to stoichiometric

Fe<sub>2</sub>(MoO<sub>4</sub>)<sub>3</sub>, and Boreskov *et al.* [7, 8] have related the activity of these systems to the coexistence of given amounts of Fe<sub>2</sub>(MoO<sub>4</sub>)<sub>3</sub> and MoO<sub>3</sub> in the catalyst, assuming that the molybdate is the active phase; similar results have been reported by Pernicone *et al.* [12]. Trifiro and coworkers have studied the redox properties of these catalysts [16] and have proposed a reaction mechanism to explain the oxidation of methanol to formaldehyde, consisting in depletion of oxygen from the catalyst lattice, thus being incorporated in the substrate molecule, and incorporation of oxygen in the lattice from the gas phase. On these grounds, the simultaneous presence of Mo<sup>6+</sup> and Fe<sup>3+</sup> in the lattice would lead to its distortion, easing the oxygen loss. In order to improve the selectivity of these catalysts, several authors have added small amounts of other trivalent cations to the catalyst [17], but the role played by these additives is far from clearly stated.

In the present paper, results are reported on the preparation and physicochemical characterization of iron-molybdenum oxide catalysts, undoped or doped with chromium. Two sets of samples have been prepared, with and without chromium, and within each series, three catalysts have been prepared with different chemical composition and Mo-Fe atomic ratios above the stoichiometric one.

## 2. Experimental details

### 2.1. Materials

The catalysts were obtained from (NH<sub>4</sub>)<sub>6</sub>Mo<sub>7</sub>O<sub>24</sub> · 4H<sub>2</sub>O and FeCl<sub>3</sub> · 6H<sub>2</sub>O (both from Merck), and Cr(NO<sub>3</sub>)<sub>3</sub> · 9H<sub>2</sub>O (Baker Chemical Co.). Gases for

\*To whom all correspondence should be addressed.

TABLE I Chemical analyses of the catalysts

Catalyst	Atomic ratio <sup>a</sup>			% weight			Atomic ratio <sup>b</sup>		
	Mo/Fe	Mo/Cr	Fe/Cr	Mo	Fe	Cr	Mo/Fe	Mo/Cr	Fe/Cr
FeMo1	0.80	–	–	53.36	13.63	–	2.28	–	–
FeMo2	1.61	–	–	55.76	11.33	–	2.86	–	–
FeMo3	3.22	–	–	57.66	9.31	–	3.61	–	–
FeMoCr1	0.80	10.04	12.50	53.70	13.08	0.47	2.39	61.91	25.91
FeMoCr2	1.61	20.09	12.50	54.82	11.92	0.62	2.68	47.94	17.90
FeMoCr3	3.22	40.18	12.50	56.75	9.65	0.44	3.42	69.92	20.43
I	–	–	–	55.88	11.75	–	2.77	–	–

<sup>a</sup>in the parent solution;

<sup>b</sup>in the solid

adsorption measurements were from S.C.O. (better than 99.99%).

## 2.2. Preparation of the samples

A known amount of  $(\text{NH}_4)_6\text{Mo}_7\text{O}_{24} \cdot 4\text{H}_2\text{O}$  (105.00, 52.50 or 26.25 g) was dissolved in 2.5 l of deionized water; a second solution was obtained dissolving 50.00 g of  $\text{FeCl}_3 \cdot 6\text{H}_2\text{O}$  in 2.5 l of deionized water; for those catalysts containing chromium, 6.00 g of  $\text{Cr}(\text{NO}_3)_3 \cdot 9\text{H}_2\text{O}$  were added to the solution containing iron. The pH was adjusted to 1.00 (pH-meter from Radiometer) with concentrated HCl (Panreac, p.a.). Both solutions were heated at 318 K and the former added to the latter, that was being thoroughly stirred, using a Mariotte flask to maintain a steady, slow addition flow; during this process, the pH was kept between 1.00 and 1.50. The precipitate was left to decant for 24 h, then filtered, washed and dried in air at room temperature and then at 398 K for 24 h. Activation of the solids was carried out by calcination in air at a heating rate of  $10 \text{ K h}^{-1}$  (Emison CH64 furnace) up to 683 K, this temperature being maintained for 2 h. The solids exhibited a greenish-yellow colour, slightly ochreous when containing chromium. The catalysts are named in Table I.

## 2.3. Catalysts characterization

Chemical analyses for molybdenum, iron and chromium were performed by atomic absorption using an EEL Mark 2-240 spectrophotometer. X-ray diffraction powder (XRD) patterns were recorded in a Jeol, mod. DX-60-S instrument, using nickel filtered  $\text{Cu K}\alpha$  radiation ( $\lambda = 154.050 \text{ pm}$ ) and standard conditions. Scanning electron micrographs (SEM) were obtained with a Philips PSEM-500 microscope. The electronic spectra of the solids in the range 850 to 220 nm were recorded with a Shimadzu UV-240 spectrophotometer provided with a diffuse reflectance accessory and a Shimadzu PR-1 graphic printer, using MgO as reference, with a slit of 5 nm.

Surface texture of the samples was monitored by adsorption of nitrogen at 77 K, using a conventional high vacuum (residual pressure less than  $10^{-4} \text{ N m}^{-2}$ ) pyrex system, provided with a rotatory pump, an oil diffusion pump and a McLeod gauge; changes in pressure were measured using a Baratron MKS pressure transducer, coupled to a KNK-202 graphic printer. Analysis of the nitrogen adsorption isotherms for specific surface area and porosity was performed with

the assistance of a BASIC programme developed by us [18] and run on a MacIntosh computer.

## 3. Results and discussion

Results of the chemical analyses of the catalysts calcined at 683 K are included in Table I, together with values for Mo–Fe, Mo–Cr, and Fe–Cr atomic ratios in the parent solutions and in the final solids.

As the Mo–Fe ratio increases in the parent solutions, the content of molybdenum in the final catalysts also does, whether or not chromium exists in the solution [19]. The method used here to precipitate the catalysts leads to solids with a very low content of the doping ion (chromium), like the findings of Alessandrini *et al.* [20], although the precipitation temperature was not the same in both cases. In addition, such a low content of chromium is favourable, as the data in the literature [17] indicate that the largest selectivity to formaldehyde is achieved with very low content of the trivalent, doping agent.

A comparison of Mo–Fe atomic ratios in the parent solutions and in the final catalysts plotted in Fig. 1,

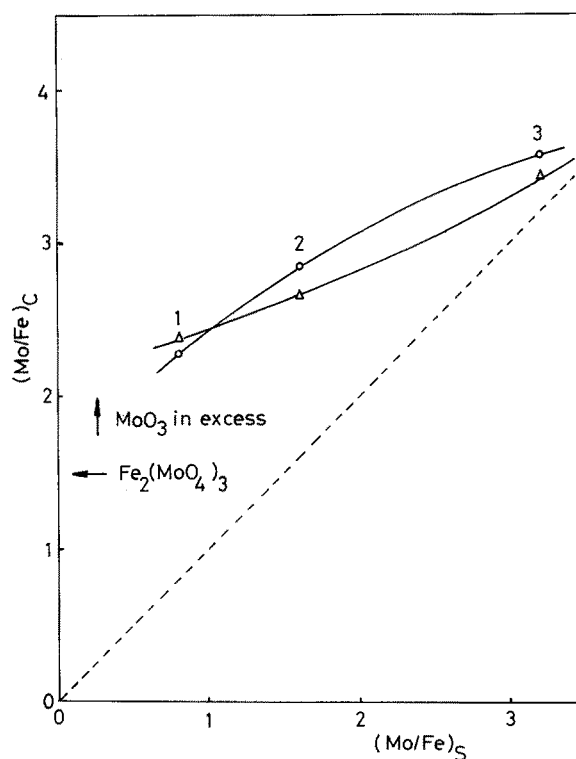


Figure 1 Atomic (Mo/Fe) ratios in the catalysts plotted against the same ratios in the parent solutions. (O FeMo,  $\Delta$  FeMoCr).

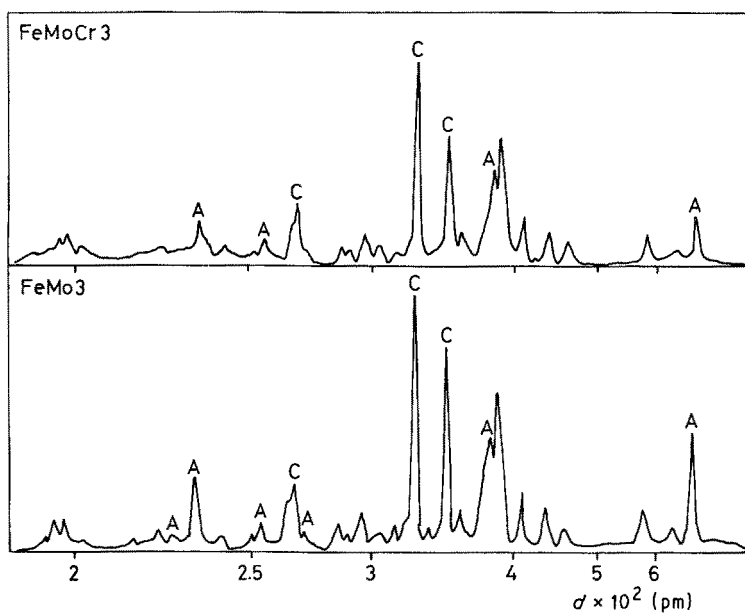


Figure 2 X-ray diffraction patterns of catalysts FeMoCr3 and FeMo3. A denotes peaks due to MoO<sub>3</sub>, C denotes peaks due to MoO<sub>3</sub> and Fe<sub>2</sub>(MoO<sub>4</sub>)<sub>3</sub>. Unlabelled peaks are due to Fe<sub>2</sub>(MoO<sub>4</sub>)<sub>3</sub>.

shows that such a ratio is lower in the former, contrary to the results reported in some patents [21]. This is probably due to the use of HCl in our solution to adjust the pH and formation of chloride-iron(III) complexes that decrease precipitation of this cation. The active species in methanol oxidation to formaldehyde has been reported to be [7, 8] iron molybdate, but with molybdenum in excess with respect to the stoichiometric value (1.5), i.e., as MoO<sub>3</sub>, our results seem to be very interesting from the economic point of view. Final catalysts with a Mo-Fe atomic ratio well above 1.5 can be obtained from parent solutions with the raw Mo-Fe  $\leq 0.80$ ; in such a case, a lower amount of heptamolybdate would be misused in the solutions after precipitation. Although more experimental data would be required, it seems that the presence of chromium does not greatly modify the Mo-Fe ratio in the final solids.

X-ray diffraction patterns for one catalyst in each series have been included in Fig. 2; similar patterns are obtained for the other catalysts, while raw solids (dried at 398 K) are amorphous. First of all, it should be noted that no peak due to Fe<sub>2</sub>O<sub>3</sub>, Cr<sub>2</sub>O<sub>3</sub>, nor Cr<sub>2</sub>(MoO<sub>4</sub>)<sub>3</sub> is detected, despite the iron content being high enough for any Fe<sub>2</sub>O<sub>3</sub> to be detected; with regards to Cr<sub>2</sub>O<sub>3</sub> or Cr<sub>2</sub>(MoO<sub>4</sub>)<sub>3</sub>, the low chromium content in our samples makes the detection of chromium species very difficult using this technique. The peaks recorded exclusively correspond to MoO<sub>3</sub> and Fe<sub>2</sub>(MoO<sub>4</sub>)<sub>3</sub> [22]. Moreover, the diffraction patterns of Cr<sub>2</sub>(MoO<sub>4</sub>)<sub>3</sub> and Fe<sub>2</sub>(MoO<sub>4</sub>)<sub>3</sub> are nearly coincident [23], as these two compounds are isostructural, and so, peaks due to Cr<sub>2</sub>(MoO<sub>4</sub>)<sub>3</sub> would be hardly detected in the presence of appreciable amounts of Fe<sub>2</sub>(MoO<sub>4</sub>)<sub>3</sub>.

Most of the peaks correspond to both MoO<sub>3</sub> and Fe<sub>2</sub>(MoO<sub>4</sub>)<sub>3</sub>, but some are ascribed to only one of these species. From the intensities of these peaks some interesting conclusions can be reached about the state of these compounds on our catalysts. The diffraction at 408 pm is due to the (012) and (021) planes of Fe<sub>2</sub>(MoO<sub>4</sub>)<sub>3</sub>. We have taken this peak as a reference, as other intense peaks of Fe<sub>2</sub>(MoO<sub>4</sub>)<sub>3</sub> overlap with peaks due to diffraction by MoO<sub>3</sub> planes. The ratio of

the intensities of peaks due to molybdena to the intensity of the peak at 408 pm due to Fe<sub>2</sub>(MoO<sub>4</sub>)<sub>3</sub>, can be tentatively taken as an indication of the relative amounts of molybdena and Fe<sub>2</sub>(MoO<sub>4</sub>)<sub>3</sub> in the solids. In Fig. 3 these values have been plotted against the

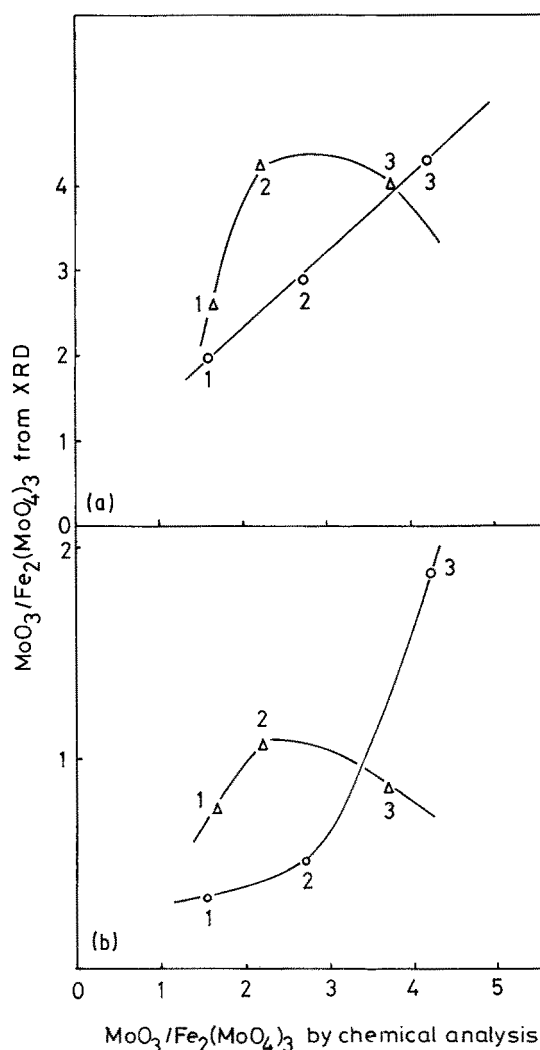


Figure 3 (a) Plot of the ratio of the intensity of the (021) peak of MoO<sub>3</sub> to the intensity of the (012) + (021) peak of Fe<sub>2</sub>(MoO<sub>4</sub>)<sub>3</sub> against the mole MoO<sub>3</sub>/Fe<sub>2</sub>(MoO<sub>4</sub>)<sub>3</sub> ratio in the solid, as calculated by chemical analysis. (b) As (a) for the (020) peak of MoO<sub>3</sub>. (O FeMo,  $\Delta$  FeMoCr).

$\text{MoO}_3/\text{Fe}_2(\text{MoO}_4)_3$  values, but obtained from the chemical analysis, assuming the absence of  $\text{Fe}_2\text{O}_3$  and  $\text{Cr}_2\text{O}_3$  (not detected by XRD) and that all chromium is present as  $\text{Cr}_2(\text{MoO}_4)_3$ . Although the presence of this compound cannot be definitely stated, it can be tentatively assumed, taking into account the excess of molybdenum (above the stoichiometric values to yield  $\text{Fe}_2(\text{MoO}_4)_3$  and  $\text{Cr}_2(\text{MoO}_4)_3$ ) existing in the samples; nevertheless, this assumption does not significantly modify the conclusions reached, due to the very low chromium content in the FeMoCr samples.

As shown in Fig. 3, diffractions by molybdena at 325 pm, (0 2 1) planes, and 690 pm, (0 2 0) planes, have been considered. Different behaviours are observed for both sets of samples (FeMo and FeMoCr) and for the intensities of both diffraction maxima. For the FeMo samples, the intensity of the (0 2 1) peak (taken as a ratio to that of  $\text{Fe}_2(\text{MoO}_4)_3$ ) increases linearly with the  $\text{MoO}_3/\text{Fe}_2(\text{MoO}_4)_3$  ratio obtained by chemical analysis. However, with respect to the peak due to the (0 2 0) planes, the intensity sharply increases for sample FeMo3. This behaviour can only be explained if it is taken into account that the intensity and sharpness of an XRD peak does not only depend on the concentration of the substance responsible for such a diffraction, but also on the size of the crystallites: the larger the crystallite in the direction perpendicular to the diffraction planes, the more intense and sharp the peak will be. Thus, the marked raising in the FeMo curve in Fig. 3b can be due to an increase in the average size of the molybdena crystallites in this sample. On the contrary, the fact that a sharp rise is not observed in Fig. 3a suggests that such a sharp (non-linear) increase in the particle size does not exist in the direction normal to the (0 2 1) planes. In other words, the  $\text{MoO}_3$  crystallites do not increase in size uniformly but anisotropically, in all directions.

A different behaviour is, however, observed with the chromium containing samples: although differences are observed from one sample to another, no simple relationship exists between the chromium content and the intensities of the molybdena peaks, however, it seems that incorporation of chromium partially cancels the anisotropic enlargement of the  $\text{MoO}_3$  crys-

tallites as the molybdenum content increases, thus favouring formation of smaller crystallites of  $\text{MoO}_3$ .

The ultraviolet-visible (UVV) spectra of the samples are very similar within a given series. Those for FeMo3 and FeMoCr3 are shown in Fig. 4. Both spectra show a very wide absorption at 200 to 400 nm that, according to data in the literature, is due to octahedral  $\text{Mo}^{6+}$  species (absorption bands at 290 to 330 nm and 225 to 240 nm) from  $\text{MoO}_3$ , and tetrahedral  $\text{Mo}^{6+}$  species (bands at 260 to 280 and 225 to 240 nm) [24] from molybdates. However, the main difference between both spectra is the increased absorption at about 500 nm in the spectrum of the chromium containing sample. This absorption is not an instrumental artifact, as it is readily recorded, but more intense, in the spectrum of a FeMoCr solid containing 1.14% (weight) chromium [25].  $\text{Cr}^{3+}$  species in an octahedral oxide environment show two spin-allowed absorption bands at 585 and 420 nm [26], i.e., the absorption recorded here lies in the middle of these absorptions and can thus be the result of the overlapping of these bands on the long wavelength side of the main absorption at 200 to 400 nm, due to  $\text{O}^{2-} \rightarrow \text{Mo}^{6+}$  charge transfer bands. A contribution to the absorption in the near UV range from the third spin-allowed transition in octahedral  $\text{Cr}^{3+}$  species cannot be absolutely ruled out.

Data on specific surface area of the samples, after calcination, have been summarized in Table II. For those catalysts without chromium, the measured specific surface area values are lower than  $1 \text{ m}^2 \text{ g}^{-1}$ ; for those containing chromium and for the commercial catalyst the values are about 7 to  $10 \text{ m}^2 \text{ g}^{-1}$ , and the corresponding  $t$ -plots [27] display positive zero-intercept, indicating the presence of micropores. Cumulative surface area values,  $S_C$ , (as obtained from Cranston and Inkley's method [28]) and surface area equivalent to adsorption on micropores ( $S_{mp}$ ), obtained following the de Boer method [27] have been also included in Table II. As expected, "external" surface area values, obtained from the slopes of the  $t$ -plots, coincide with the  $S_C$  values. While samples FeMoCr2 and FeMoCr3 have similar  $S_{BET}$  values, nearly coincident with that for the commercial catalyst, the value for sample FeMoCr1 is about 35% lower. At first it seems that the presence of chromium avoids collapsing of the structure of the precursor solids, like the results reported by Alessandrini *et al.* [20] with Fe-Mo-Bi-O systems. Obviously, this does not apply to the commercial catalyst, with a similar  $S_{BET}$  value, despite the absence of chromium, probably due to the patent-protected method used to obtain it.

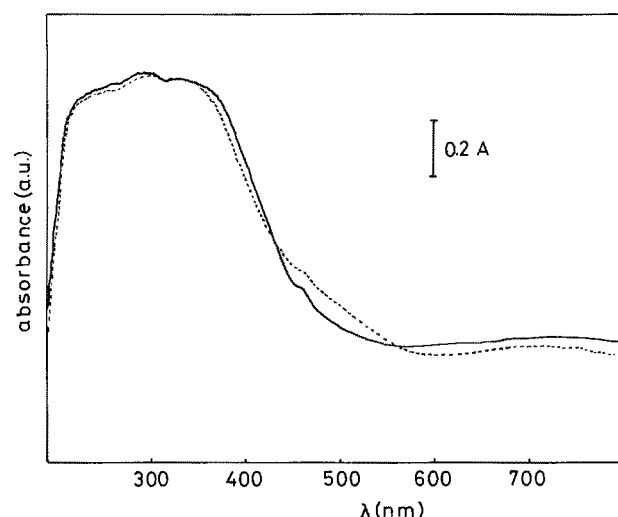


Figure 4 Electronic spectra (diffuse reflectance) of catalysts FeMo3 (solid line) and FeMoCr3 (dotted line). References: MgO.

TABLE II Specific surface area values ( $\text{m}^2 \text{ g}^{-1}$ ) for the catalysts

Catalyst	$S_{BET}$	$S_C$	$S_{mp}$
FeMo1	$\approx 1$	—	—
FeMo2	$\approx 1$	—	—
FeMo3	$\approx 1$	—	—
FeMoCr1	6.9	3.8	2.6
FeMoCr2	10.4	6.4	4.8
FeMoCr3	10.8	6.4	4.3
I	10.3	7.8	2.4

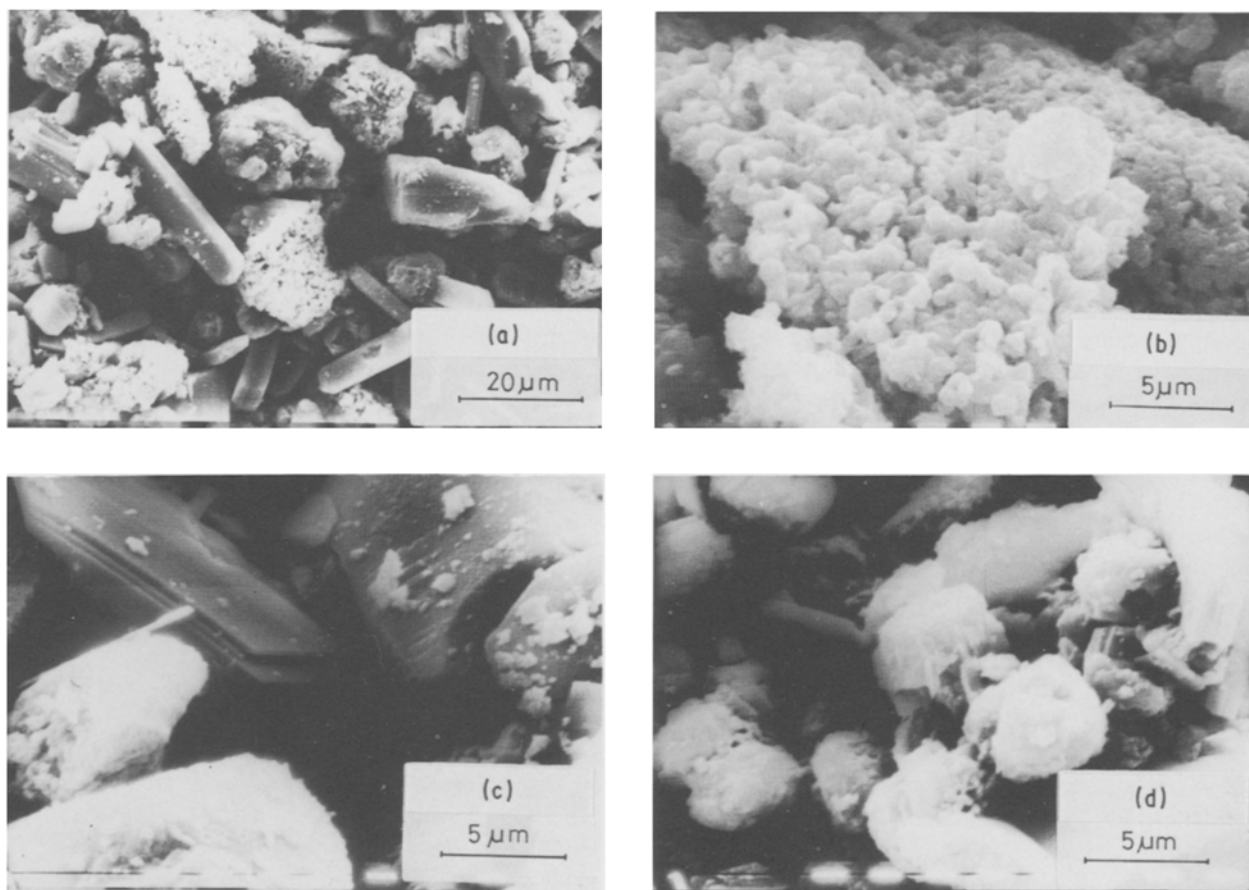


Figure 5 Scanning electron micrographs of catalyst FeMo3 (a and b) and FeMoCr3 (c and d).

Nevertheless, no simple relationship can be stated between the chromium content and the  $S_{\text{BET}}$  values: it seems that the mere presence of chromium is enough to develop larger specific surface areas (see values for samples FeMo and for samples FeMoCr). Again, the behaviour of catalyst I is somewhat peculiar, with an appreciable  $S_{\text{BET}}$  value, probably due to the preparation method, as this catalyst does not contain chromium.

Finally, it should be noted that external surface area values (coincident with  $S_{\text{C}}$ ) represent  $58 \pm 3\%$  of  $S_{\text{BET}}$  in all three FeMoCr samples; we have not found any reason for this result. It should also be mentioned that pore size distribution curves were very similar for all FeMoCr and I catalysts, with a maximum around 2 nm; however, a second, lower, maximum at about 3.3 nm decreases in intensity as the molybdenum content in the sample is increased (FeMoCr1 < FeMoCr2 < FeMoCr3), while for the commercial catalyst a wider distribution of pore size in the range 2 to 6 nm is observed.

Scanning electron micrographs for two samples, one with and another without chromium, are shown in Fig. 5. For sample FeMo3, Fig. 5a, two types of crystals are found: stick-type crystals, corresponding to molybdena [20], and sponge-like crystals, identified as  $\text{Fe}_2(\text{MoO}_4)_3$ . On the contrary, for sample FeMoCr3, Fig. 5c, the presence of chromium leads to pillared lamellar crystals; with a largest content of chromium [25], the formation of such plate-like particles is even more evident.

The presence of chromium seems to modify the

topology of both  $\text{MoO}_3$  and  $\text{Fe}_2(\text{MoO}_4)_3$ , even with very low chromium content, thus accounting for the noticeable increase in the specific surface area of FeMoCr samples. The whole set of micrographs in Fig. 5 shows these changes: with Fig. 5a (FeMo3) and Fig. 5c (FeMoCr3), the change in the topology of the molybdena crystals is observed, as described above, while Fig. 5b (FeMo3) and 5d (FeMoCr3) show a great change in the shape of the  $\text{Fe}_2(\text{MoO}_4)_3$  crystals, that seem to be the result of agglomeration of compact particles in FeMo3, but in sample FeMoCr3 the appearance is more flaky, with lamellar crystals forming rose-like groups.

#### 4. Conclusions

From the work carried out so far, some very interesting conclusions can be reached about the optimum way to synthesize chromium-doped, iron molybdenum oxide catalysts for methanol oxidation to formaldehyde. The chemical composition of the FeMo and FeMoCr catalysts depend on the relative concentrations of iron and molybdenum salts in the parent solutions, and, to a lesser extent, on the presence of chromium. In addition, texture properties are also modified, the specific surface area increases, and microporosity develops.

#### References

1. I. MAATSUURA, S. MIZUNO and H. HASHIBA, *Polyhedron* **5** (1986) 111.
2. U. OZKAN and G. L. SCHRADER, *J. Catal.* **95** (1985) 120, 137, 147.
3. K. BRÜCKMAN, R. GRABOWSKI, J. HABER,

- A. MAZURKIEWICZ, J. SLOCZYNSKY and T. WILTOWSKI, *ibid.* **104** (1987) 71.
4. J. HABER and E. SERWICKA, *Polyhedron* **5** (1986) 107.
  5. J. F. LA PAGE, J. COSYNS, P. COURTY, E. FREUND, J. P. FRANK, Y. JACQUIN, JUGUIN, C. MARCILLY, G. MARTINO, J. MIGUEL, R. MONTARNAL, A. SUGIER and H. van LANDEGHEM, "Catalyse de Contact", (Technip, Paris, 1978).
  6. M. DENTE, R. POPPI, I. PSAQUON, *Chim. Ind. (Milan)*, **46** (1964) 1326.
  7. G. K. BORESKOV, G. D. KOLOVERTNOV, G. L. M. KEFELI, L. M. PLYASOVA, KARAKCHIEV, V. N. MASTIKIN, B. I. POPOV, V. A. DZISKO and D. V. TaARASOVA, *Kinetika i Kataliz. (Engl. Trans.)*, **7** (1966) 144.
  8. G. K. BORESKOV and G. D. KOLOVERTNOV, *ibid.* **6** (1966) 1052.
  9. A. ADKINS and W. R. PETERSON, *J. Amer. Chem. Soc.* **53** (1931) 1512.
  10. R. Y. KHOKHLER, L. N. KUDRINA and N. V. KUDRINA, *Izv. Vyssh. Uchebn. Zaved. Khim. Tekhnol.* **25** (1982) 710.
  11. T. POPOV, V. BANCHEVA and S. KRUSTEV, *Heterog. Katal. (Engl. Trans.)*, **2** (1983) 181.
  12. N. PERNICONE, G. LIBERTI and L. ERSINI, *Proceedings 4th International Congress Catalysis, Moscow* (1968), Rice University Printing, Houston, 1969, paper no. 21.
  13. T. YANG and J. H. LUNSFORD, *J. Catal.* **103** (1987) 55.
  14. T. ONO, M. ANPO, Y. KUBOKAWA, *J. Phys. Chem.* **90** (1986) 4780.
  15. A. R. NEFEDOVA, Z. V. GRYAZNOVA, Z. I. YAKOVENKO and A. T. KHUDIEV, *Vestn. Mosk. Univ. Ser. 2, Khim. (Engl. Trans.)* **22** (1981) 490.
  16. F. TRIFIRO, V. de VECCHI and I. PASQUON, *J. Catal.* **15** (1969) 8.
  17. P. COURTY, H. AJOT and B. DELMON, *C. R. Acad. Sci. Paris (C)* (1973) 1147.
  18. C. MARTIN, V. RIVES and P. MALET, *Powder Technol.* **46** (1986) 1.
  19. A. M. ESTEVEZ SANCHEZ, A. FERNANDEZ TENA and M. A. PORTILLO CEBALLOS, Spanish Patent 550 187 (1986).
  20. G. ALESSANDRINI, P. CARIATI, P. FURZATTI, P. L. VILLA and F. TRIFIRO, "2nd International Conference on Chemistry & Uses of Molybdenum" edited by P. C. H. Mitchell and A. Seeman (Climax Molybdenum Co. Ltd, London, 1976) 186.
  21. P. MELOCCHI, (Montecatini S.G.I.M.C.), Italian Patent 599 419 (1959).
  22. J.C.P.D.S. 5-0508, 20-256.
  23. L. M. PLYASOVA and L. M. KEFELI, *Neorganicheskie Materialy, (Engl. Trans.)* **3** (1977) 906.
  24. F. E. MASSOTH, *Adv. Catal.* **27** (1978) 265.
  25. M. del ARCO, C. MARTIN, V. RIVES, A. M. ESTEVEZ and A. F. TENA, *Reactivity of Solids*, submitted for publication.
  26. A. B. P. LEVER, "Inorganic Electronic Spectroscopy" 2nd edn. (Elsevier, New York, 1984) p. 417.
  27. B. C. LIPPENS and J. H. de BOER, *J. Catal.* **4** (1965) 319.
  28. R. W. CRANSTON and F. A. INKLEY, *Adv. Catal.* **9** (1957) 143.

Received 8 June  
and accepted 1 November 1988